Application of a statistical vortex generator model approach on the short-chord flap of a three-element airfoil

F. VON STILLFRIED[a], S. WALLIN[a,b] and A. V. JOHANSSON[a]
[a] Royal Institute of Technology Stockholm
Linné Flow Centre
Department of Mechanics
SE - 100 44 Stockholm, Sweden

[b] Swedish Defence Research Agency
Computational Physics
SE - 164 90 Stockholm, Sweden

florian@mech.kth.se, stefan.wallin@foi.se, johansson@mech.kth.se

Summary

Current flap designs on civil transport-type aircraft comprise approximately 30% of the undeployed wing chord. The objective of the short-chord flap project HELIX (Innovative aerodynamic high lift concepts, 2001-2005) within the Fifth framework programe by the European Commission was to reduce the trailing edge flaps to 20% chord or less. The benefits of such a short-flap airfoil are e.g. increased fuel tank capacity within the wing, weight savings due to lighter flap track fairings and drag reduction during cruise flight. The major challenge for a short-chord flap airfoil to overcome is the higher flap deflection angle during take-off and landing phases in order to maintain the same amount of lift as for an airfoil with conventional flap size. Flow control devices such as stationary passive vortex generators (VGs) that are mounted on such a short-chord flap can alleviate or even totally avoid flow separation at high deflection angles.
A sound computational fluid dynamics investigation of such a flow case requires an adequate grid with a corresponding large number of grid points around such VGs in order to obtain an accurate solution. This, in turn, leads to a time-demanding grid generation which often comes along with lots of practical challenges during the creation. An effective way to get around this time-consuming process is to introduce a modeling of the VGs and to add their physical effects to the governing equations rather than resolving their geometries in the computational grid. FOI, the Swedish Defence Research Agency, and KTH, the Royal Institute of Technology Stockholm, have developed computational tools for VG modeling that make it possible to simulate and to add the additional physical effects of modeled VGs in wall-bounded flows whereas the need for a local mesh refinement in the vicinity of such modeled VGs is no longer required. A method to statistically model VGs is presented and applied in this paper. Experimental and computational results are compared for the HELIX short-chord airfoil take-off configuration for different VG model parameter settings.

1 Introduction

The operational envelope in aeronautical and other engineering designs is in many cases limited by turbulent boundary layer separation. The possibility of controlling and delaying the separation enables more efficient designs that can be used for improving the performance or for optimizing the design in order to reduce drag and weight. Turbulent boundary layers can be energized by introducing vortices by vortex generators (VGs) that increase the mixing of momentum in the boundary layer and, by that, increase the near-wall velocity. Experimental studies as well as computations have shown the ability of controlling separation with such devices.
Lin [7] provides a review of the research activities in the field of passive low profile VGs. Basic fluid dynamics and applied aerodynamics research of the performance enhancement of various flow cases due to low profile VGs is presented. Low profile VGs are most efficient when flow separation is relatively fixed and they produce "minimal near-wall protuberances" in order to overcome flow separation. The height of such low profile VGs is typically around $0.1 \leq h/\delta_{99} \leq 0.5$

which in turn reduces drag compared to larger VGs but still ensures the low profile VGs acting as highly effective control devices against flow separation compared to conventional designs. Lin states that the nondimensional geometrical device parameters such as the VG chord to height ratio c/h and the VG pair distance to height ratio D/h are increased substantially when the height h is reduced, leading to different geometrical properties than in classical design guidelines for conventional VGs. At the same time, angles of incidence α should be increased to ensure sufficient vortex strength when LPVGs are used for flow separation control.

In computational fluid dynamics (CFD), the most straightforward way to mimic VGs is to fully resolve their geometry within the mesh. This leads to very fine meshes in the vicinity of such VG structures in order to resolve the developing boundary layer on the VG vane surface as well as the developing vortex structures in its vicinity and further downstream. Thus, fully resolved VGs lead to rather high computational costs.

Another way to take VGs into account is rather modeling the resulting effects of VGs in a flow field. This approach removes the need to mesh the VG geometry. Jirásek [6] describes two types of different models for mimicing VGs: a vortex source model, and a lifting force model. The vortex source model needs a user input such as the initial circulation of the VGs according to the Biot-Savart law. The lifting force model, developed by Bender, Anderson and Yagle [2] and generally called BAY model, rather uses the lifting force that is generated by the VGs and estimated by the lifting line theory (LLT), see e.g. [4]. The lifting force is added to the Navier-Stokes equations and therefore acts directly on the flow and, by that, forms vortices. Jirásek also presents a new so-called jBAY model that is developed from the BAY model. The jBAY model removes some of the shortcomings of the BAY model such as the lack to model the effects of multiple VGs and the difficulty to define the grid points where the model should be applied.

A statistical VG model approach was introduced in [8]. This model approach describes the statistical effects of VGs on the flow. Here, the vortex flow field is derived by only taking the geometrical properties of VGs into account, inspired by [11]. The circulation distribution Γ(y) across one VG blade is needed as an input for the VG modeling and is estimated by the lifting line theory (LTT), see e.g. [4], or [1]. Then, the resulting cross stream vortex velocity field is added indirectly by means of the second order statistics of the generated vortex velocity field in a small region through forcing terms in a Reynolds stress transport (RST) model. Furthermore, the drag generation of the modeled VGs is considered by added volume forces in the streamwise component of the momentum equation. An advantage of this method is that no mesh refinement is needed and that the computational costs compare solely with solving the Reynolds averaged Navier-Stokes (RANS) equations, thus, enabling design and optimization of VG settings by CFD.

Investigations of this statistical VG model in a zero pressure gradient (ZPG) boundary layer flow over a flat plate are presented in [9]. The investigation has shown that the statistical modeling of VGs was effectually deployed and truly has the advantage of not being more computational expensive than solving RANS equations.

The main objective of this work is to examine the capabilities of the statistical VG model in adverse pressure gradient (APG) flow over a short-chord flap of a three-element airfoil. The clean three-element airfoil at take-off configuration was investigated at a rather high angle of attack. Second, the two dimensional (2D) VG model was introduced at this angle of attack on the suction side of the short-chord flap. This investigation included a parameter variation study of the modeled geometry such as the VG height, chord and shape plus the position of the VG model plane.

2 Analytical and numerical methods

The modeling of the VGs in this investigation follows the way suggested in [8] who presented a model that requires neither mesh refinements nor 3D computations. In this model approach, the VGs are represented by a vortex source model that uses the lifting line theory in order to estimate the generation of circulation by the VGs. The circulation distribution Γ(y) across a wing according to the LLT is given by

$$\Gamma(y) = \frac{K}{2} U(y) c(y) \left[\alpha(y) - \frac{w(y)}{U(y)} \right], \tag{1}$$

where K is the local section lift slope of the wing (K_{max} = 2π rad^{-1} according to thin airfoil theory), U(y) is the local incoming free stream velocity, c(y) the local chord length of the wing, α(y) the local angle of attack, and w(y) the local downwash due to the trailing vortex sheets. The ratio w(y)/U(y) is the local induced angle of attack α_{ind}(y) for small angles α, and the local downwash w(y) reads

$$w(y) = \frac{1}{4\pi} \int_{-h}^{h} \frac{d\Gamma}{dy'} \frac{1}{y' - y} dy'. \tag{2}$$

Equations (1) and (2) are solved by means of a Fourier series ansatz, see e.g. [1]. The LLT holds for high aspect ratio (AR) wings in free flight conditions for small angles of attack α far away from obstacles in the flow. By modeling VGs that are mounted on a wall in a boundary layer flow by means of the LLT, some of its original assumptions are not valid anymore as a result of:

- a boundary layer velocity profile U(y) instead of a constant free stream velocity U_∞,
- VGs being very low AR wings,
- possible side effects due to the proximity of neighbouring VG blades, i.e. neighbouring vortices,
- a reasonable high angle of incidence α (corresponding the angle of attack α for free flight in the LLT) of the VG blades.

Therefore, the LLT is only used as an approximation to estimate the circulation distribution Γ(y) across a single VG blade. In turn, the circulation distribution Γ(y) quantitatively describes the generated lift, the induced drag and the vortex strength which is again needed as an input for the vortex model. The vortices are then represented by a Lamb-Oseen vortex model with the azimuthal velocity distribution

$$u_\Phi(r) = \frac{\Gamma_{max}}{2\pi r}\left[1 - \exp\left(\frac{-r^2}{r_0^2}\right)\right], \tag{3}$$

where Γ_{max} is the maximum value of the circulation distribution Γ(y), determined from the LLT (see Eq. (1)), r_0 the vortex core radius and r the radial coordinate from the vortex center. A limitation of this 2D vortex model is that the velocity component in the streamwise direction is constant.
A VG array consists of more than one VG so that all VGs influence the vortex flow field everywhere in the VG model plane[1] at the streamwise position $x_{VG,mod}$ from the flap leading edge. Due to that, a superposition of the vortex induced velocities u_Φ(r) for each VG and their corresponding blades was needed. The wall acts approximately as a symmetry condition for the vortices, which is simulated by introducing mirror vortices.
The concept of this VG model approach and describing its effects on the flow is to assume that the second order statistics of the additional vortex velocity field act like additional Reynolds stresses on the mean flow. By making this assumption, the additional spanwise averaged contributions $\Delta\overline{u_i'u_j'}$(y) to the Reynolds stresses are

$$\Delta\overline{u_i'u_j'}(y) = \frac{1}{D}\int_{-D/2}^{D/2} u_i'(y,z)u_j'(y,z)dz. \tag{4}$$

It is sufficient to integrate and spanwise average the second order statistics in Eq. (4) over one VG pair distance D since the resulting vortex flow field is periodic. Additional contributions from Eq. (4) are only nonzero for $\Delta\overline{v'v'}$ and $\Delta\overline{w'w'}$. Moreover, a wall damping function, e.g. (1-exp(-20y/h)), needed to be introduced and applied on Eq. (4) because the vortex velocities in the spanwise direction at the wall boundary y = 0 will not cancel out and would result in a finite value in Eq. (4).
After applying the additional vortex stresses, a RST turbulence model was used to properly describe the development of the total Reynolds stresses downstream of the VG plane. Furthermore and unlike simpler turbulence models, a RST turbulence model makes it possible to account for the energy transfer between the different components of the Reynolds stress tensor, thus enabling production of the important shear layer $\overline{u'v'}$ Reynolds stresses.

3 Experimental setup

In a previous study within the HELIX project, various short-chord flap designs with different shroud lengths were investigated. Finally, the short-chord flap design in Figure 1 was chosen for contiuative studies. The objective was to experimentally substantiate the performance predictions from previous studies, in particular since the performance enhancement by flow separation control devices was estimated by means of ealier experiences with sub-boundary layer VGs for separation control.
Experiments including a conventional three-element airfoil with a standard chord length (baseline geometry) and the new airfoil geometry with a 20% short-chord flap were carried out by VZLU, the Czech Institute of Aviation. An open jet, closed-return, low-speed wind tunnel was used and 2D end-plate models of the baseline and the short-chord geometries were manufactured. These models allowed a variation in slat and flap deflections as well as a variation of flap lap and flap gap positions relative to the main element. Both, the baseline and the short-chord flap configurations were optimised in terms of the flap lap and gap position.
Generally, the investigations encompassed an angle of attack range from α = -5° to +30° and surface pressure measurements at 20% model semi-span were made for 13 baseline and 7 short-chord flap configurations by means of 128 pressure

[1]Throughout this paper, the VG model plane is assumed to be the corresponding yz-plane at the streamwise trailing edge location of the modeled VGs.

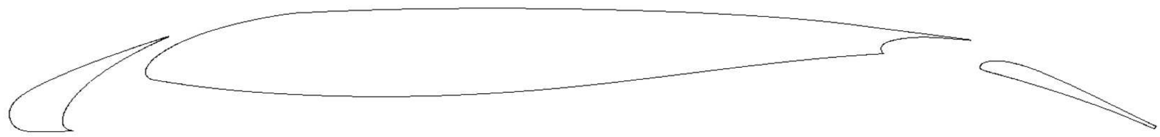

Figure 1: The HELIX short-chord three-element airfoil geometry.

holes. The Reynolds number for all experiments was $1.65 \cdot 10^6$ based on the undeployed baseline chord c_{base} and the freestream Mach number was Ma_∞ = 0.13.
In particular, the short-chord flap flow control experiments for takeoff and landing configurations were carried out with delta shape vane-type sub-boundary layer VGs attached at 25% flap chord c_{flap} in a co-rotating configuration with a height h_{VG}, a chord c_{VG}, positioned with a d_{VG} spanwise spacing at an angle of incidence α_{VG} towards the freestream direction. In experiments, the flap deflection angle δ_F of the short-chord flap was increased by 50% for the takeoff and by 0%, 8% and 23% for the landing configuration compared to the baseline configuration in order to match baseline performance results.
The experiments have shown that the short-chord flap in takeoff configuration with flow control devices attached could provide the lift performance of the baseline takeoff configuration even though the maximum lift coefficient $C_{L,max}$ could not be achieved. Therefore, the ability of the short-chord flap to replace the baseline configuration in takeoff configuration was partly shown. The remaining part of this paper investigates only the short-chord flap takeoff configuration in order to evaluate the statistical VG model against the experimental results with flow control devices.

4 Computational set-up

The circular computational domain included the HELIX airfoil in its center, surrounded by ca. 70000 nodes. The circular shape made it possible to change the angle of attack by means of the free stream velocity components without taking additional boundary conditions into account as for a rectangular domain. The mesh around the airfoil was kept fine in region of high flow curvatures, i.e. especially in the vicinity of the two gaps between the three airfoil elements. The near wall grid points were located at $y^+ = \mathcal{O}(1)$ in order to ensure capturing the viscous effects close to the wall. Yet, there is potential to increase the mesh density in the wall normal direction in order to resolve the near wall effects better. However, the mesh was fine enough for such an investigations that was rather examining the trends of such a VG model approach rather than matching experimental results quantitatively.
Valid throughout this paper, the HELIX airfoil computations were carried out using a differential Reynolds stress model (DRSM) as a turbulence model with pressure-strain rate model corresponding to the Wallin & Johansson explicit algebraic Reynolds stress model (EARSM) with curvature correction, see [10]. This DRSM was also linked with the Hellsten k-ω turbulence model from [5]. The DRSM turbulence model was applied since the VG model was written for a usage in combination with DRSM models, adding the additional vortex stresses directly to the governing equations.
Corresponding to experiments, the Reynolds number based on c_{base} and the Mach number were set to $Re = 1.65 \cdot 10^6$ and $Ma = 0.13$, respectively.

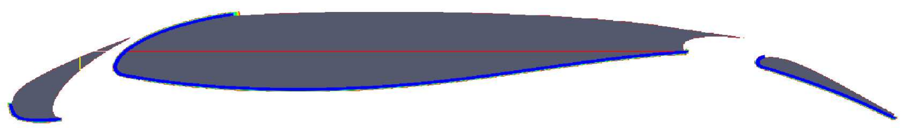

Figure 2: Laminar regions (blue) on the airfoil element surfaces.

First, test computations without the VG model applied were carried out with fully turbulent flow as well as with pre-defined transition regions on the airfoil element surfaces since Re was rather low and the position of the transition point is an important aspect that neither has been triggered nor measured nor estimated. The purpose of this rather ad-hoc procedure was to match the experimental C_P results without VGs better than with fully turbulent flow. Figure 2 shows the laminar regions colored in blue on the three elements for a high angle of attack whereas the transition setting is also based on previous experience on similar cases. The analogous C_P distribution results are given in Figure 3. Here, it can be

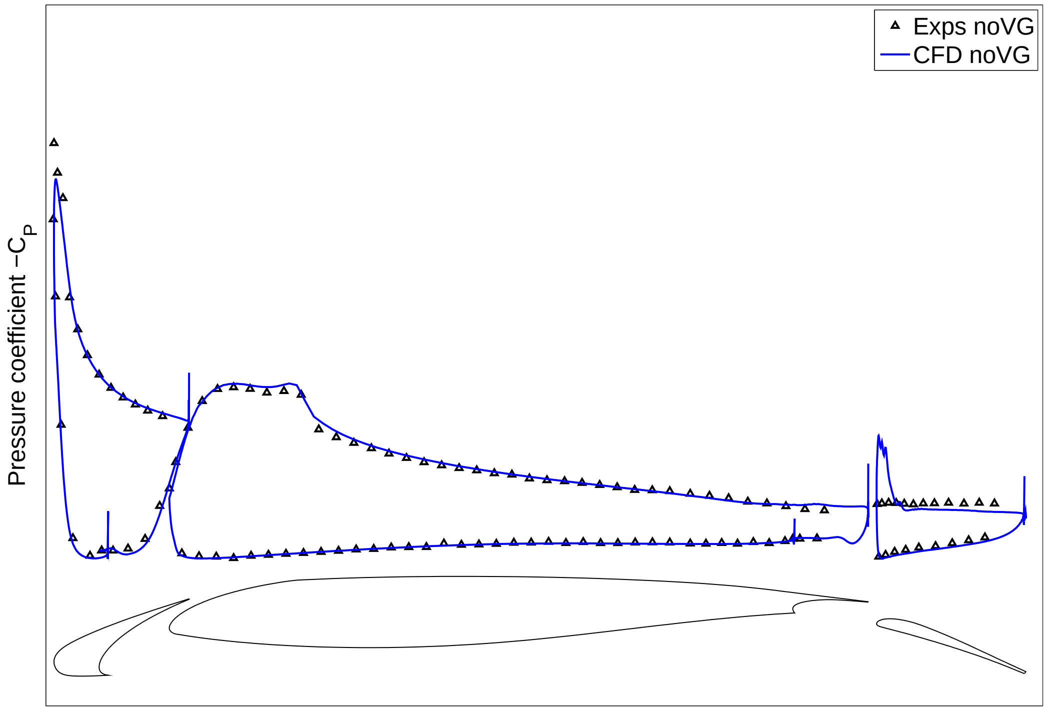

Figure 3: C_P distribution plots of experiments and CFD without VGs, fully turbulent and transition settings used.

seen how the blue curve for the computations with transition settings reproduces experimental results with high accuracy. Nevertheless, it is conspicuous that the C_P distribution around the flap shows a peak value close to the flap leading edge. This characteristic is a result of the non-converged steady RANS computations that also indicate the shedding vortices in time whereas the experimental data represent a time-averaged flow regime. The result of introducing the laminar regions was very promising and the laminar/turbulent transition settings were therefore also applied for the flow cases with the VG model.

Second, computations including the statistical VG model were carried out for a range of high angles of attack when separation occurs on the flap. This part of the investigations included a VG model parameter variation of its corresponding modeled VG geometry in terms of shape, chord length, height and VG model position. These input parameter can be simply set in a preprocessing step, keeping the original mesh without the need of any mesh refinement. In particular, all computations were carried out with the Edge CFD code [3] and for all runs, the lift slope factor K in Eq. 1 was set to $1.8 \cdot \pi$ rad^{-1}, i.e. 10% lower than for the thin airfoil theory.

5 Results

This chapter presents the experimental data with and without attached flow control devices and the computational results with applied VG model. Previous runs have shown that the original experimental set-up including the VG configuration did not lead to separation prevention in computations when the VG model was applied. At this streamwise position, i.e. at 25% c_{flap}, the VG model plane was consequently placed in the mean flow separation region where the model cannot have any effect on the mean flow characteristics. Unlike in computations, such an experimental set-up can lead to separation prevention due to the fact that the flow around the flap device is fluctuating and therefore flow around the VGs is temporarily attached. This can be effectual to generate the needed vortex structures that ensure boundary layer mixing and hence keep the flow attached.

It was chosen to move the VG model plane further upstream in order to place it in a smaller as well as permantly attached boundary layer where the VG model can successfully create the necessary vortex stress forcing terms that act on the mean flow. Moreover, parameter variations of the modeled geometry including the modeled VG height, chord length and shape

Table 1: Positions and configuration settings of VG model on the HELIX short-chord flap.

$x_{VG,mod}/c_{flap}$	4%				8%			
$c_{VG,mod}/c_{VG,exp}$	50%				100%			
$h_{VG,mod}/h_{VG,exp}$	100%		150%		100%		150%	
Shape	▲	■	▲	■	▲	■	▲	■
Configuration	1	2	3	4	5	6	7	8

as well as of the VG model plane position were carried out. The parameters and their corresponding values related to the experimental set-up are given in Table 1.

Figure 4 displays streamline plots including velocity magnitudes in the vicinity of the main element trailing edge and the flap for the same angle of attack. The comparison clearly shows the differences between the clean and the modified short-chord flap airfoil, here with VG model configuration 8. Furthermore, Figures 5 and 6 show the resulting C_P plots of this investigation that include C_P distributions for all computations from in Table 1.

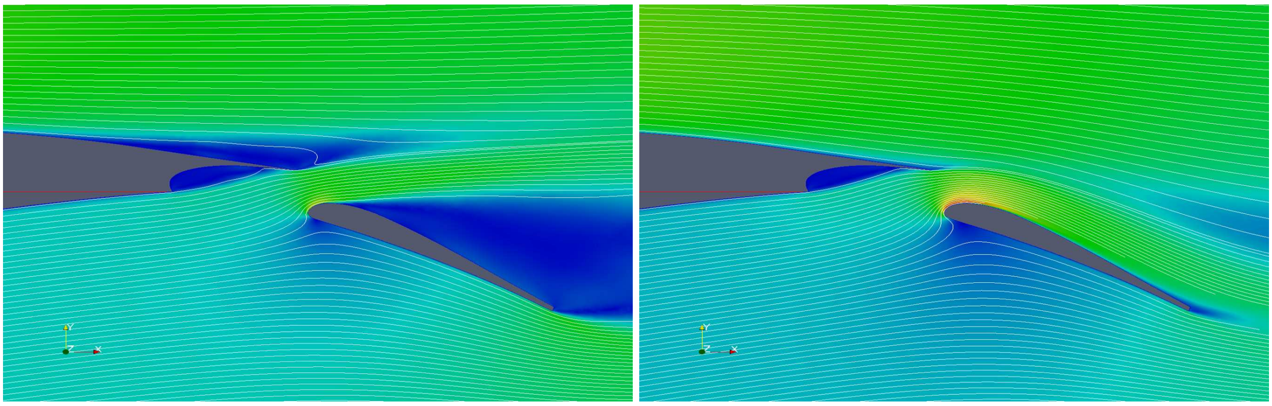

a) b)

Figure 4: Velocity magnitude (blue: low velocity; red: high velocity) and streamline plots for a) the clean airfoil without VG model; b) the modified airfoil with the VG model configuration 8 applied: x_{VG}/c_{flap} = 8%, $c_{VG,mod}/c_{VG,exp}$ = 100%, h_{VG} = 150%, rectangular shape.

5.1 VG model variation

5.1.1 Plane variation

Figure 5 presents the different examined VG models with configuration setting 1-4, located at 4% c_{flap} in addition to the experimental results with VGs attached at 25% flap chord. Here, it can be observed that the VG model configurations 1-3 describe almost the same C_P curves on all three elements. Configuration 4 with larger rectangular modeled VGs shows a visible decrease of C_P on the suction side of all airfoil elements leading to a fully attached flow on the flap. It should be mentioned that the VG model is located very close to the laminar/turbulent transition point. Figure 6 shows the corresponding curves at 8% c_{flap}, yet with another value for the modeled VG chord $c_{VG,mod}/c_{VG,exp}$ = 100% rather than 50% as in the previous case. The reason for the smaller chord was to ensure that the modeled real VG chord did not exceed the leading edge of the flap. The particular effect of different chord lengths will be analyzed separately in upcoming investigations. However, Figure 6 generally shows how the overall peak pressure distribution is decreased on the flap. This might be the consequence of the double chord length that leads to a higher Γ_{max} in Equation 1. Moreover, two out of four configurations show almost congruent C_P distributions, compared to only one configuration that fully ensured separation prevention on the flap. This shows that the VG model position plays a role for an optimization of the mixing effects of flow separation prevention devices.

5.1.2 Height variation

The VG model height has a major influence on the effectiveness of flow separation prevention as can be seen in Figure 6. There, a higher VG model is preventing the mean flow from separation, compare configurations 5 and 7 as well as 6 and 8 with each other. This is a result of the fact that the higher the VG model, the higher are the velocites around the wing tip and the higher gets Γ_{max} in Equation 1, leading to larger additional forcing terms in the RANS equations. Under certain circumstances when this height difference is of relative importance it can have a non-negligible impact on the mean flow field, leading to potential flow separation prevention.

5.1.3 Shape variation

Figures 5 and 6 show that the modeled VG shape can lead to differences in the C_P distribution, depending on where the VG model plane is located and how tall the modeled VG is. Figure 5 displays C_P distribution plots for the different VG model configurations for the further upstream located VG model plane location at 4% c_{flap}. There, configurations 3 and 4, representing delta and rectangular modeled VGs, respectively, prove to illustrate that the differences regarding a flow separation prevention are considerable. The configurations 1 and 2 do not show this sensitivity but, for this case, it is presumed that the VG model height has more importance on results than the modeled shape. Figure 6 does not to show any sensitivities in the C_P distributions at all for a shape variation, the small differences for configurations 5 and 6 occur from the non-converged steady computations, giving different flow states as a result of the fluctuating and separated flow region on the flap.

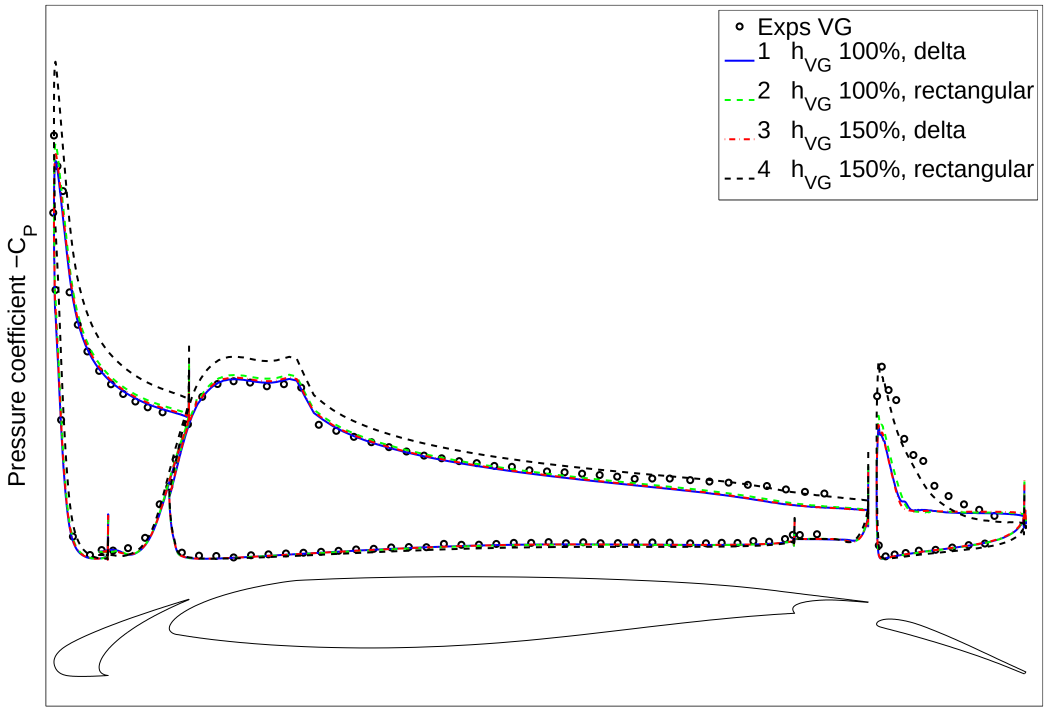

Figure 5: C_P distribution plots: experiments with VGs at 25% c_{base} and computations with different VG model configurations 1-4, see Table 1. The VG model plane is located at $x_{VG,mod}/c_{flap}$ = 4% with a modeled chord length of $c_{VG,mod}/c_{VG,exp}$ = 50%.

6 Conclusions

This investigation has shown the capabilities of the application of a statistical VG model approach on the short-chord flap of the HELIX three-element airfoil to mimic the effects of co-rotating VG arrays by means of introducing additional statistical vortex stresses to the governing mean flow equations.

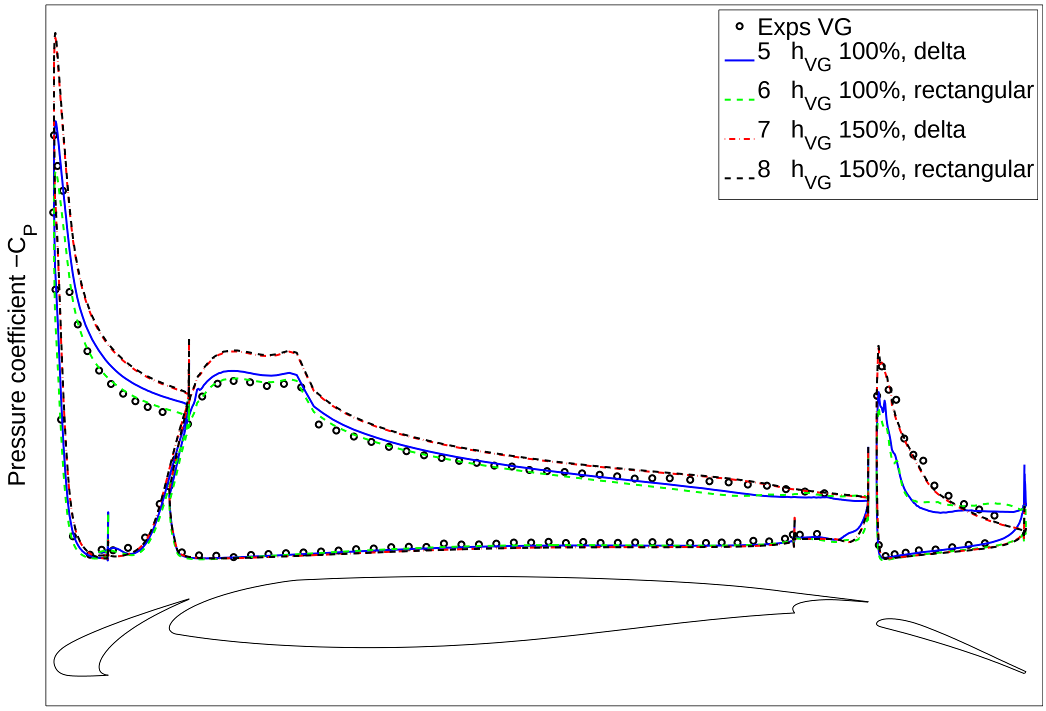

Figure 6: C_P distribution plots: experiments with VGs at 25% c_{base} and computations with different VG model configurations 5-8, see Table 1. The VG model plane is located at $x_{VG,mod}/c_{flap}$ = 8% with a modeled chord length of $c_{VG,mod}/c_{VG,exp}$ = 100%.

Pressure distribution plots and images of the instantaneous flow regime around the three-element airfoil illustrate that the VG model computations successfully improve the flow by means of preventing separated flow on the flap for certain VG model configurations. In particular, Figures 5 and 6 show the C_P distributions for the VG model parameter study (see also Table 1). There, the effect of configurations 4, 7 and 8 on successfully preventing flow separation is clearly visible. Furthermore, the trends and tendencies show that the statistical VG model approach shows sensitivity for different VG model heights, shapes and forcing plane locations. From the examined cases, it can be concluded that all VG model parameters have an effect on the flow, yet with different importance. Especially the VG height and VG model plane position are more relevant than the actual shape of the VG model even though Figure 5 shows some sensitivity according to a delta/rectangular shape variation. Further investigations including the modeled VG shape and chord will be carried out in future in order to draw more consolidated conclusions from these independent VG model parameter.
In total it can be said that this investigation has shown that the statistical VG model approach is very promising for an application on airfoils and has the advantage of not being more computational expensive than solving RANS equations without modeled VGs, leading to much faster results than with conventional methods such as fully or partly resolved VGs.

Acknowledgements

The experimental data are originated from the EC 5th Framework programme HELIX, GRDI-2000-25205. This project was supervised by Simon Galpin of Airbus-UK. Special thanks to Ulf Tengzelius of FOI for his help and comments regarding the HELIX project.

References

[1] J. D. Anderson. *Fundamentals of Aerodynamics*. McGraw-Hill, 2nd edn., 1991.

[2] E. E. Bender, B. H. Anderson, and P. J. Yagle. "Vortex generator modelling for Navier-Stokes codes." *American Society of Mechanical Engineers*, 1999. FEDSM 99-6919.

[3] P. Eliasson. "Edge, a Navier-Stokes solver for unstructured grids." *Proceedings to Finite Volumes for Complex Applications III*, 2002:pp. 527–534. Edited by D. Kroner and R. Herbin, Hemre Penton Science London.

[4] H. Glauert. *The Elements of Aerofoil and Airscrew Theory*. Cambridge University Press, London, UK, 1st edn., 1926.

[5] A. Hellsten. "New advanced k-ω turbulence model for high-lift aerodynamics." *AIAA Journal*, 2005. 43(9):pp. 1857–1869.

[6] A. Jirásek. "A vortex generator model and its application to flow control." *Progress in Aerospace Sciences*, 2005. 38(4-5):pp. 389–420.

[7] J. C. Lin. "Review of research on low-profile vortex generators to control boundary-layer separation." *Progress in Aerospace Sciences*, 2002. 38(4-5):pp. 389–420.

[8] O. Törnblom and A. V. Johansson. "A Reynolds Stress Closure Description of Separation Control With Vortex Generators in a Plane Asymmetric Diffuser." *Physics of Fluids*, 2007. 19(115108).

[9] F. von Stillfried, S. Wallin, and A. V. Johansson. "Statistical modeling of the influence of turbulent flow separation control devices." *47th AIAA Aerospace Sciences Meeting, Orlando, Florida*, 2009. AIAA 2009-1501.

[10] S. Wallin and A. V. Johansson. "Modelling Streamline Curvature Effects in Explicit Algebraic Reynolds Stress Turbulence Models." *International Journal of Heat and Fluid Flow*, 2002. 23(5):pp. 721–730.

[11] B. J. Wendt. "Initial Circulation and Peak Vorticity Behavior of Vortices shed from Airfoil Vortex Generators." Tech. rep., NASA, 2001.